HEFT

D2.4. Analysis and validation of machine insulation for 800V DC bus

Funded by
the European Union

Call	HORIZON- CL5-2020-D5-01	
GA Number	101096306	
Deliverable No.	D2.4	
Deliverable Title	Analysis and validation of machine insulation for 800V DC bus	
Deliverable Date	2024-06-21	
Contractual delivery	2024-03-31	
Deliverable Type	R	
Dissemination level	PU	
Status	V2.0	2024-06-21

Written By	Andrea Cavallini	2024-03-19
Checked by	Fernando Garramiola	2024-05-16
Approved by	Javier Poza	2024-06-21

HORIZON CL5-2020-D5-01. HEFT 101096306 – Novel concept of a Low Cost, High Power Density and Highly Efficient Recyclable motor for next generation mass produced electric vehicles

Acknowledgement:

The author(s) would like to thank the partners in the project for their valuable comments on previous drafts and for performing the review.

Project partners:

MGEP (Mondragon Goi Eskola Politeknikoa Jose Maria Arizmendiarrieta S Coop).
GKN (GKN Driveline Zumaia SA).
GKN AIC (GKN Automotive Innovation Center - GKN Hybrid Power Ltd.).
MAGNETI (Magneti Ljubljana d.d.).
VYNCOLIT (Vyncolit N.V.).
IKERLAN (IKERLAN S. Coop.).
UNIBO (Alma Mater Studiorum - Università di Bologna).
KUL (Katholieke Universiteit Leuven).
UoN (University of Nottingham).

TABLE OF CONTENTS

LIST OF FIGURES

LIST OF TABLES

GLOSSARY

Abbreviation/ acronym	Description
CR-PAI	Corona-resistant Polyamide-imide
FEA	Finite Element Analysis
HV	High Voltage
IEC	International Electrotechnical Commission
GKN	GKN Driveline Zumaia Sa
OF	Overshoot Factor
PAI	Polyamide-imide
PD	Partial Discharges
PDIV	Partial Discharge Inception Voltage
SUMIBE	Sumitomo Belgium
UNIBO	University of Bologna

REFERENCES

[1] IEC Std. 60034-18-41, Rotating electrical machines - Part 18-41: Partial discharge free electrical insulation systems (Type I) used in rotating electrical machines fed from voltage converters - Qualification and quality control tests. 2019.

[2] LV123, Electrical Characteristics and Electrical Safety of High-Voltage Components in Road Vehicles.

[3] 61857-42, Electrical insulation systems - Procedures for thermal evaluation - Part 42: Specific requirements for evaluation of an electrical insulation system (EIS) used for road transportation applications.

[4] M. Pastura et al., “Partial Discharges in Electrical Machines for the More Electric Aircraft—Part I: A Comprehensive Modeling Tool for the Characterization of Electric Drives Based on Fast Switching Semiconductors,” IEEE Access, vol. 9, pp. 27109–27121, 2021, doi: 10.1109/ACCESS.2021.3058083.

1 EXECUTIVE SUMMARY

In this document the insulation system of the HEFT motor is discussed. In particular, the following points will be explained:

A. **Evaluation of voltage stresses**. The voltage stresses in the phase-to-phase, phase-to-ground, and turn-to-turn insulation system are evaluated based on:
    a. Guidelines provided in [1].
    b. Estimation of turn voltage distribution based on FEA (see Appendix)
B. **Definition of target partial discharge inception voltages (PDIV)**. Based on the expected operating conditions of HEFT machine and the voltage stress calculated in A, target levels for the PDIV of the different insulation sub-systems are defined.
C. **Reference insulation system.** The insulation system to be used (enamels, resins) is discussed. The insulation thickness of conductors is estimated from previous experience.
D. **Characterization of slot molding resins.** The dielectric behavior of innovative slot molding resins (provided by SUMIBE) at different frequencies and different temperatures is discussed. Among a set of four candidate resins, two are selected for further evaluation.
E. **Assessment of phase-to-phase insulation system**. The phase-to-phase insulation system in the end-winding is the weakest point of the system. The safety margins (defined as the PDIV minus voltage in operation) are experimentally evaluated at high temperatures, using an insulation model aimed at reproducing the features of the end-winding.
F. **Assessment of phase-to-ground insulation system**. Similar to E, but for the phase-to-ground insulation. Conservative results are presented, neglecting the additional insulation layer of slot molding which will be used to separate conductors from the stator in the HEFT e-motors.
G. **Assessment of turn-to-turn insulation system**. Similar to E, but for the turn-to-turn insulation.
H. **Chemical compatibility**. The goal is to establish the compatibility of the resin, and enamel with the chosen lubricant oil.

2 MAIN ASSUMPTIONS FOR DESIGN

The main assumptions for design were agreed upon by GKN and UNIBO.

- Based on WP4 specifications about conductor temperature (≤180°C), the insulation of the conductors will be based on polyamide-imide, with a temperature class of 220°C.
- The supplier for preliminary testing will be Ederfil Becker (https://www.ederfilbecker.com/). It is suggested that Ederfil Becker will also be the supplier for the machines.
- Calculations of the minimum partial discharge inception voltage (PDIV) of the insulation was based on [1].
- The winding is full pitch, so conductors of different phases will not be within the same slot. Nevertheless, the most critical part of the insulation is the phase-to-phase insulation in the end-winding, where conductors from different phases can be separated by a micrometric gap.
- Owing to the above point, the primary insulation (enamel) should be designed to withstand the phase-to-phase voltage without incepting partial discharges.
- Based on [2], the maximum DC bus voltage in operation is assumed to be the rated DC bus voltage of the system (i.e., 800 V); it is assumed that the maximum DC bus voltage will not exceed this value as the inverter overvoltage protection (*crowbar*) will not allow exceeding this value to protect the switches.
- The DC bus voltage is assumed to be bipolar with respect to the frame of the machine, that is, if the worst case is, for instance, 800 V, the pole voltages of the DC bus will be ± 400 V.
- The overshoot factor (ratio between peak voltage at machine terminals and DC bus voltage) was assumed to be equal to 1.2, based on measurements performed by GKN.
- The temperature enhancement factor [1] has been taken relatively high ($EF_{temp} = 1.2$) despite the fact that the end-windings (critical part of the insulation system) will be oil cooled.
- The enhancement factor for aging [1] has been neglected ($EF_{aging} = 1$) considering that:
    - the average temperature in service will be normally lower than the hot spot as the maximum power will be rarely used,
    - the class temperature of the insulation will be 220°C: much higher than the hot spot temperature (180°C),
    - the target lifetime (10,000 hours),

3 ESTIMATION OF ELECTRICAL STRESS APPLIED TO THE INSULATION SYSTEM

Calculations were based on the standard IEC 60034-18-41 [1] when dealing with the enhancement (safety) factor that would ensure the reliability of the system. Indeed, the selected insulation system (PAI), in the absence of chemical compatibility issues, would age as predicted by [1]. The calculations of the stress voltages depart from the guidelines proposed in [1] to reflect the differences existing between industrial and automotive drives. The equations reported below were agreed upon during the preparation of [3] by the responsible of UNIBO (Andrea Cavallini) in his role of project leader of the second edition of [1], and members of IEC TC 112 WG 6 in charge of preparing [3].

Table 3-1. Drive specifications

Parameter	Symbol	Value	Units
Number of levels	n	2	-
DC bus voltage design value	U_{des}	800 1000 1200	(V)
Overshoot Factor	OF	1.2	-
Turn-to-turn voltage to jump voltage ratio at 30 ns (calculations based on Section 11)	ρ	0.19	-

Table 3-2. Voltage stress calculations (peak-to-peak voltages)

Voltage	Equation (based on [1])	Value @ U_{des}=800V	Value @ U_{des}=100V	Value @ U_{des}=1200 V	Units
Voltage overshoot	$\mathrm{U}_b = (\mathrm{OF} - 1) \times \frac{U_{des}}{n-1}$	160	200	240	(Vpk/pk)
Phase-to-phase	$U_{P-P} = 2 \times (U_{des} + U_b)$	1920	2400	2880	(Vpk/pk)
Phase-to-ground	$U_{P-G} = U_{des} + 2 \times U_b$	1120	1400	1680	(Vpk/pk)
Turn-to-turn	$U_{T-T} = 2 \times \frac{2}{3} \times \rho \times (U_{des} + U_b)$	243	304	364	(Vpk/pk)

Table 3-3. Temperature specifications

Temperature	Value	Units
Class temperature	220	(°C)
Service temperature	180	(°C)

Table 3-4.Enhancement factors [1]

Factor	Enhancement factor	Selected value
Temperature	Range: 1.0-1.3	1.2
Thermal aging	$EF_{aging} = \max\left(1.2 \frac{\text{Service temperature}}{\text{Class temperature}}, 1\right) = \max(0.98, 1)$	1
PDIV/PDEV hysteresis	Not considered as the DC bus voltage used for calculation is the maximum possible in operation.	1

Table 3-5.Test voltages for type tests

Insulation system	Service voltages (Vpk/pk)	EF Temp.	EF Aging	Test voltages (Vpk/pk)
Udes = 800 V				
Phase-to-phase	1920	1.2	1	2304
Phase-to-ground	1120	1.2	1	1344
Udes = 1000 V				
Phase-to-phase	2400	1.2	1	2880
Phase-to-ground	1400	1.2	1	1680
Udes = 1200 V				
Phase-to-phase	2880	1.2	1	3456
Phase-to-ground	1680	1.2	1	2016

4 VALIDATION AND SELECTION OF SLOT OVER-MOLDING RESIN

4.1 Preliminary screening of alternative candidates

SUMIBE developed an alternative to slot liners based on the idea of injecting in the slot epoxy resin loaded with conductive particles, thus creating a thermally conductive slot over-molding. The process requires a special injector as sketched in Figure 4-1.

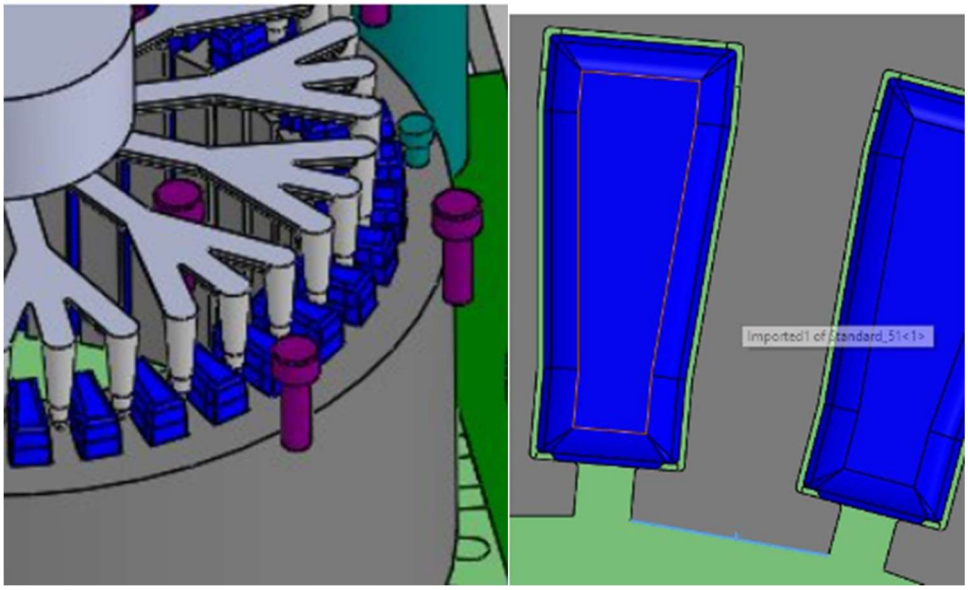

Figure 4-1. SUMIBE resin injection process

For HEFT, SUMIBE proposed four candidate resins:

- G720E
- M200
- XP8474
- XQ8763

UNIBO carried out dielectric spectroscopy and weight loss measurements on samples of these candidate resins. The samples were measured:

1. As received
2. After 10 days in the oven at 180°C
3. After further 30 days in the oven at 200°C

The first measurements performed on the sample were dielectric spectroscopy measurements at temperatures from -20°C to 180°C and frequencies from 10^{-1} Hz to 10^{7} Hz. The results are summarized in Figs. Figure 4-2 - Figure 4-4.

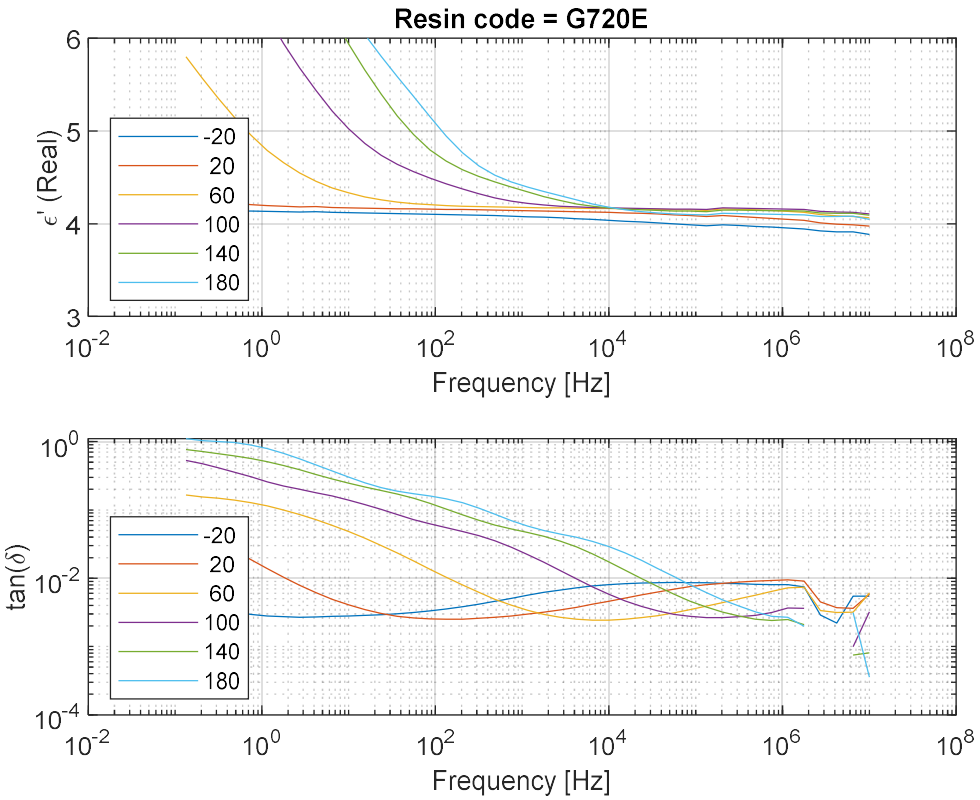

Figure 4-2. Dielectric spectroscopy of resin G720E

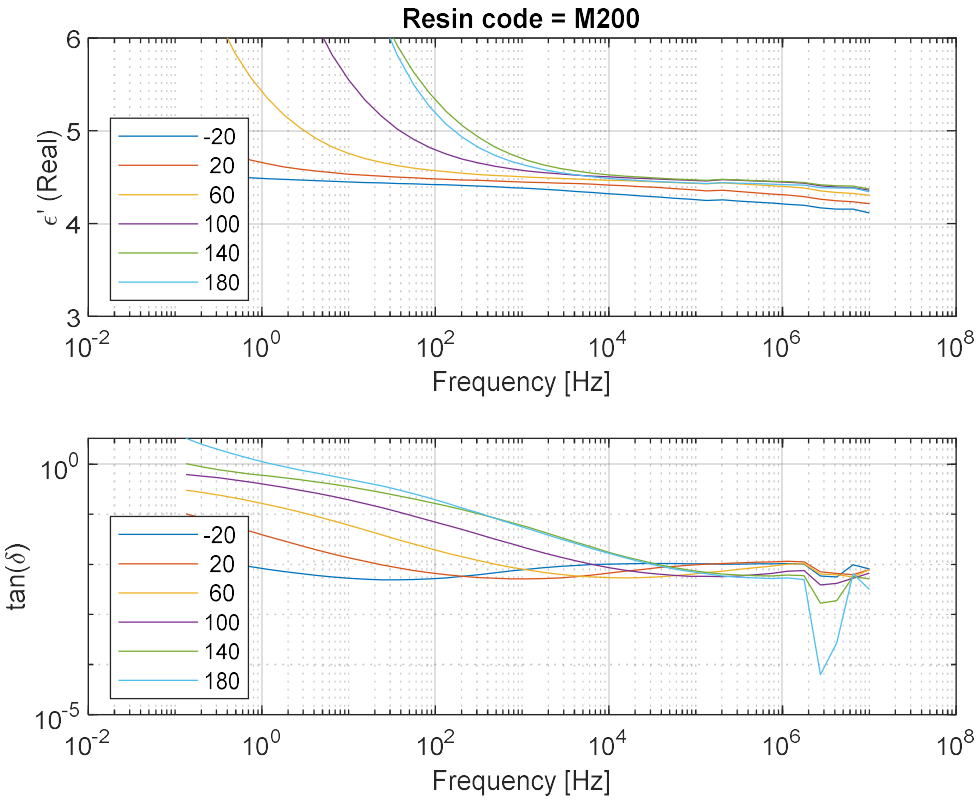

Figure 4-3. Dielectric spectroscopy of resin M200

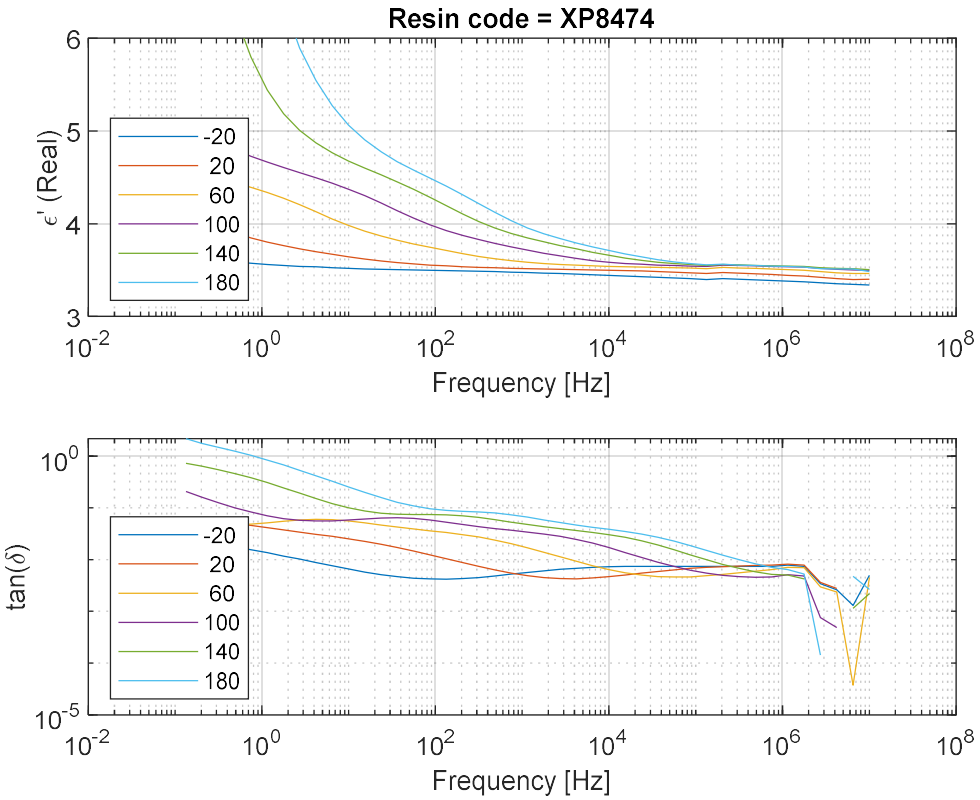

Figure 4-4. Dielectric spectroscopy of resin XP8474

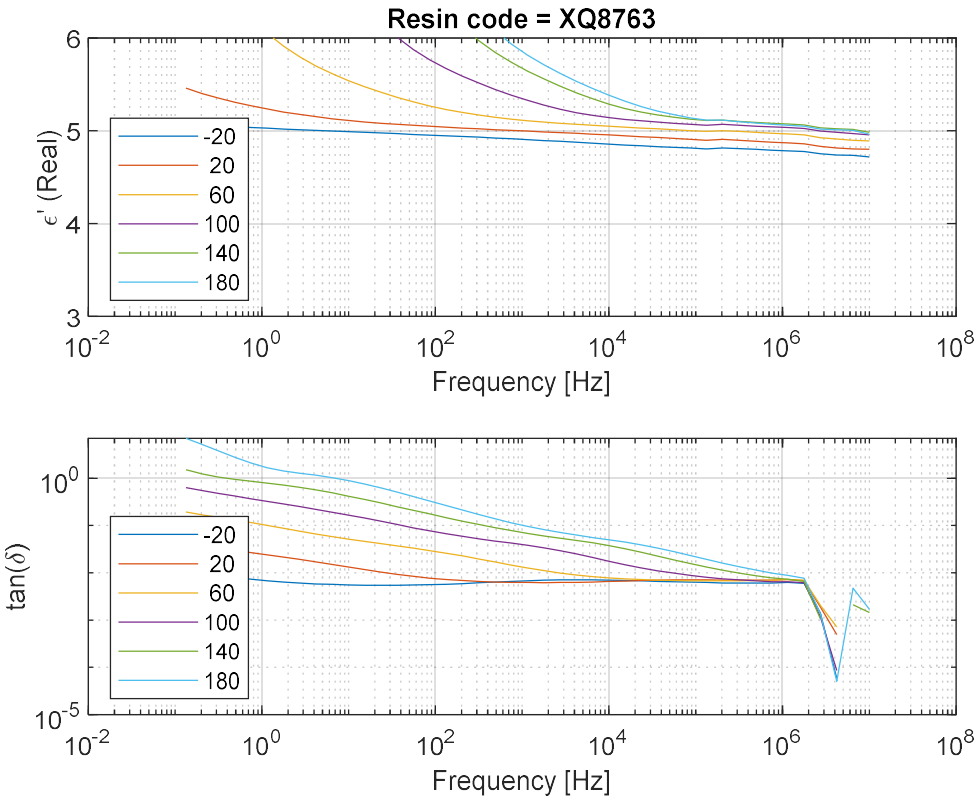

Figure 4-5. Dielectric spectroscopy of resin XP8474

In order to summarize the measurements in a somewhat easier framework, the results of dielectric spectroscopy at 1000 Hz, with the samples having a temperature of 180°C, are reported in Table 4-1. Note that 180°C is the maximum temperature of the stator, the worst case in terms of permittivity (higher permittivity favoring the inception of partial discharges) and dielectric dissipation factor (higher dielectric losses, possibly leading to overheating and, in the worst case, thermal runaway). A summary of the results is reported in Table 4-1. As can be seen, candidate resins can be roughly divided in two groups:

A. Resins G720E and M200: these resins present a higher stability of the permittivity and a lower dissipation factor. However, their weight loss is slightly higher.
B. Resins XP8474 and XQ8763: these resins have lower weight losses but higher permittivity and dissipation factor.

Table 4-1.Results of dielectric spectroscopy carried out on SUMIBE resins

NAME	Real part of relative permittivity (ε') @ 1 kHz, 180°C			Loss factor, $tan(\delta)$ @ 1 kHz, 180°C			Weight loss (%)
	As received	10d @ 180°C	30d @ 200°C	As received	10d @ 180°C	30d @ 200°C	30d @ 200°C
G720E	4.4	4.2	4.2	0.058	0.015	0.003	1.234
M200	4.6	4.3	4.3	0.051	0.0076	0.007	1.672
XP8474	3.9	3.6	4.2	0.066	0.028	0.020	0.913
XQ8763	5.8	5.2	5.1	0.096	0.032	0.022	0.969

Considering results on electrical properties, the best resin is G720E. This resin has also an intermediate weight loss, so it could be a good compromise.

Alternatively, the resin XQ8763, which has excellent thermal properties, could be also a valid alternative despite a larger permittivity that could be promoting partial discharge inception. Indeed, considering the results reported in Section 6, it was concluded that this resin is a valid option for systems at 800 V and 1000 V, whereas further analysis with complete models is needed for 1200 V.

Accordingly, both G720E and XQ8763 were considered for the next step, that is, the assessment of their compatibility with the lubricant oil used for cooling.

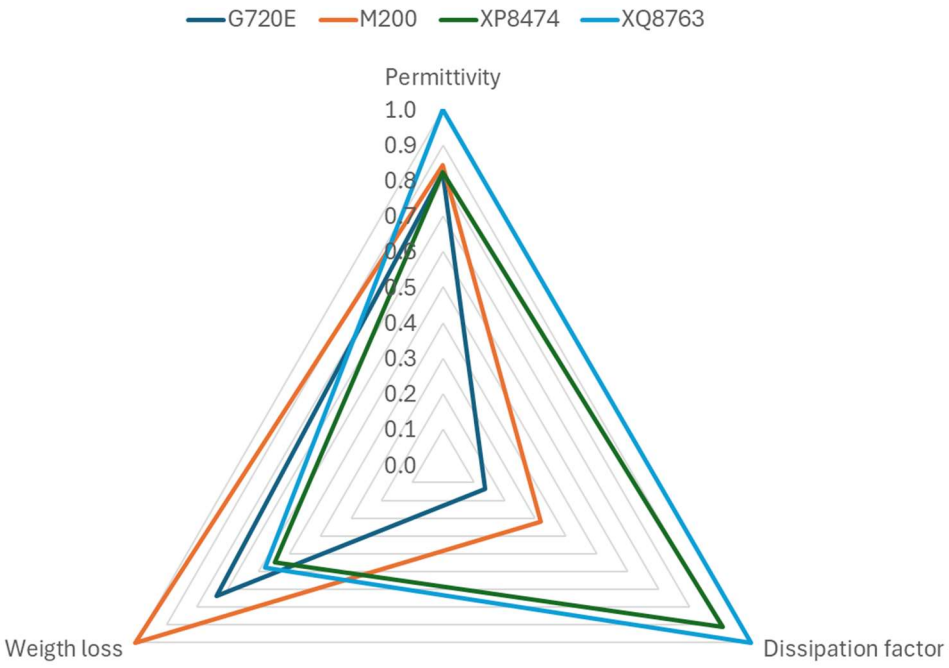

Figure 4-6. Radar plot of resin properties (all values have been normalized to the maximum value observed across the various candidate resins). The smaller the triangle the better is the resin.

5 ASSESSMENT OF PHASE/PHASE INSULATION

5.1 Preliminary choice of conductor insulation

The selection of the insulation thickness for the conductor was based on the worst case, i.e., the phase-to-phase insulation. The voltages for type tests reported in Table 3-5 were used as a reference. These voltages, designated for testing under ambient temperature conditions, were directly compared with PDIV data collected from both UNIBO and GKN tests on circular and rectangular conductors (see Figure 5-1). Comparing the target values in Table 3-5 and the PDIV data in Figure 5-1, the insulation thickness of the conductor was estimated, as shown in Table 5-1.

Table 5-1.Preliminary estimates of conductor insulation thickness

DC bus voltage, U_{des} (V)	Reference PDIV ($V_{peak/peak}$)	Thickness (μm)
800	2304	≥90
1000	2880	≥120
1200	3456	≥150

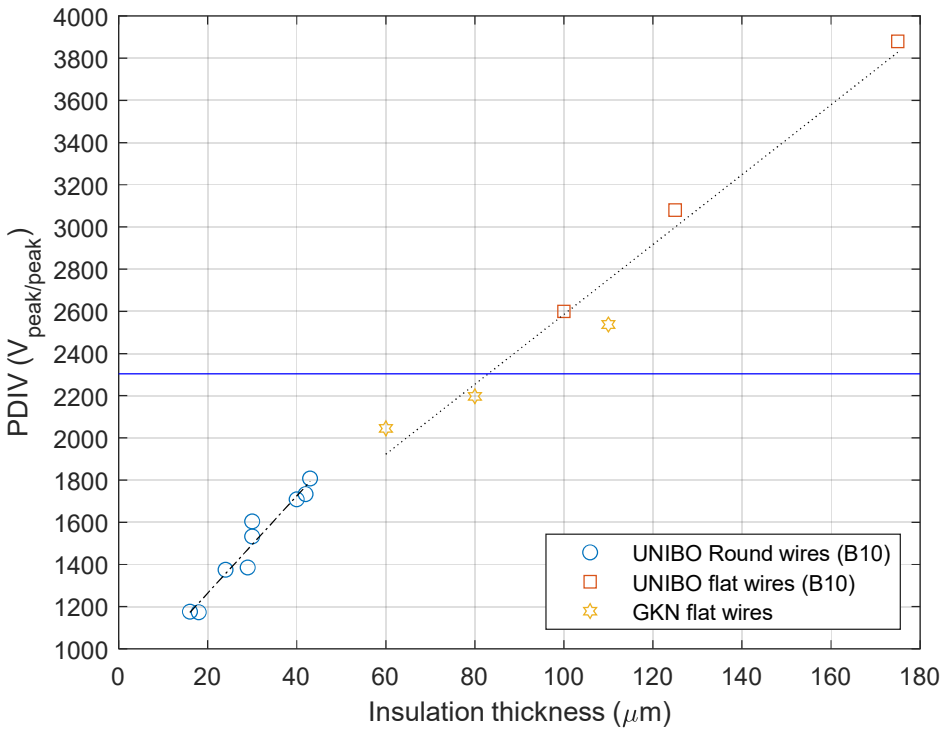

Figure 5-1. PDIV data based on UNIBO and GKN data combined. Peak-to-peak voltages.

5.2 Conductors chosen for the tests and insulation models

Considering the market offer, the suppliers of both UNOT and GKN, rectangular conductors having an insulation thickness of 80 μm and 110 μm were first investigated. Both Polyamide-Imide (PAI) and corona resistant PAI (CR-PAI) were considered.

Since the HEFT winding will be full pitch, conductor of different phases will not be in intimate contact within the slots. Therefore, parallel conductors separated by air gaps representing the conductor arrangement in the end-winding were considered. The insulation models are reported in Figure 5-2. As can be seen, it is not easy to make the conductors perfectly parallel in the middle of the insulation model (where the gap is the lowest and the partial discharge inception probability the highest). Therefore, it was checked that at least the minimum distance between the conductors was equal to the air gap length selected for testing.

Tests were carried out at different temperatures in the oven. Therefore, the conductor holders in Figure 5-2 were realized using MACOR (machinable glass ceramic), which is known to be highly stable up to 800°C and with minimal thermal expansion coefficient (assembly was done at room temperature, test were performed up to 180°C).

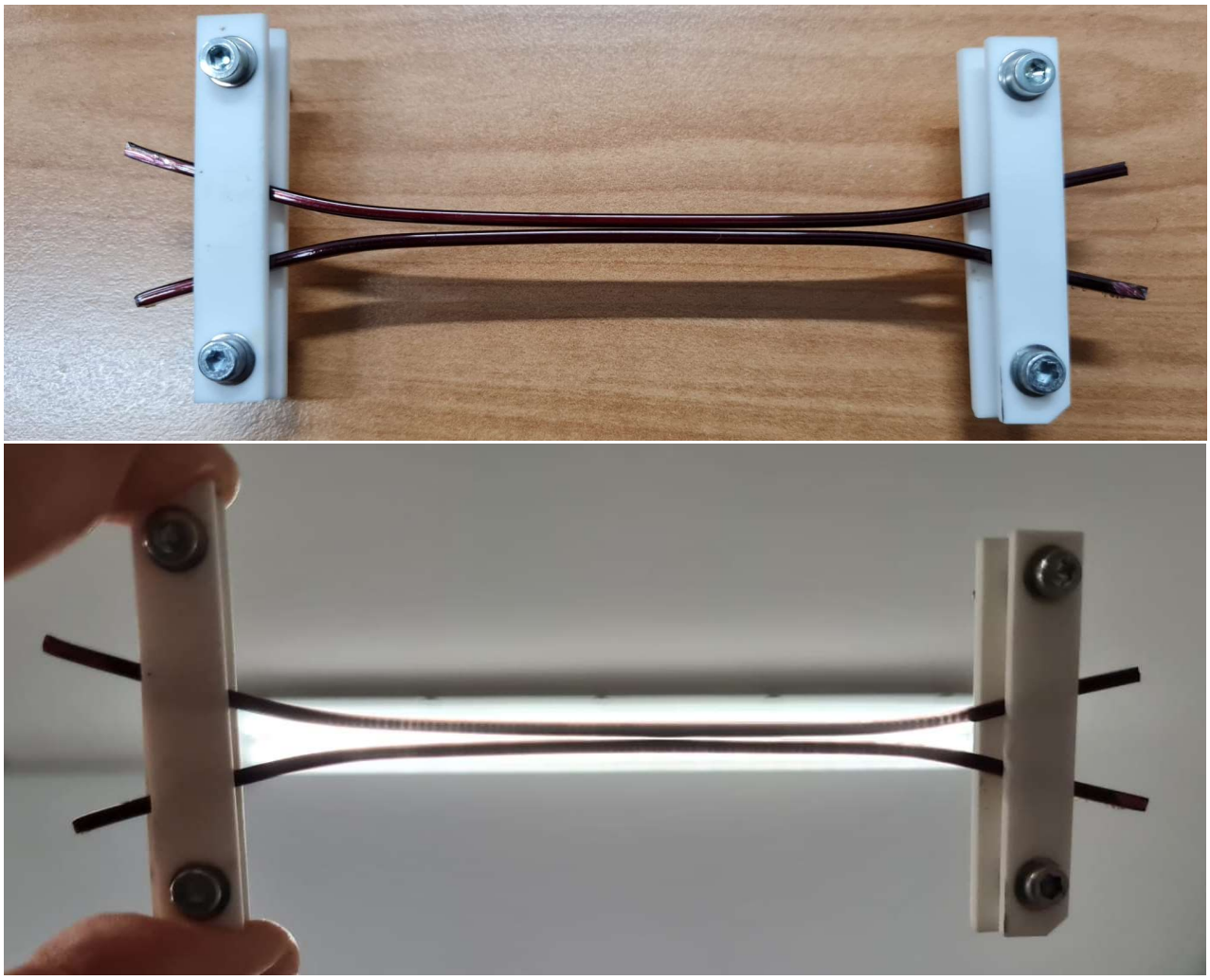

Figure 5-2. Insulation models for testing the phase-to-phase PDIV in the end-winding.

5.3 Temperature and gap dependence of PDIV

5.4 Insulation thickness 110 μm

In the first place, the behavior of the conductors having 110 μm-thick insulation was investigated. This conductor is the one with the highest likelihood of being the final one (the conductor having 80 μm thick insulation is below the expectations reported in Table 5-1 for the 800 V bus. The results are reported in Figure 5-3. The results show that:

a. PDIV decreases monotonically with temperature. This result was expected as temperature decreases the density of the air. To a lesser extent, it can modify the permittivity of the material. However, as the glass transition temperature of PAI is normally larger than 180°C, this effect is negligible.
b. CR-PAI is loaded with ceramic nanoparticles of undisclosed nature and weight content. Yet, as ceramics have typically permittivity much larger than the base resin (~4 versus ~10), it might be that the permittivity of CR-PAI is larger, explaining why the PDIV of CR-PAI is generally lower.
c. As the temperature increases, the PDIV gap between PAI and CR-PAI is partially reduced, making CR-PAI attractive despite its poorer performance at ambient temperature.

Considering the monotone behavior of PDIV on temperature, test for the conductors having 80 μm-thick insulation were carried out at 180°C only.

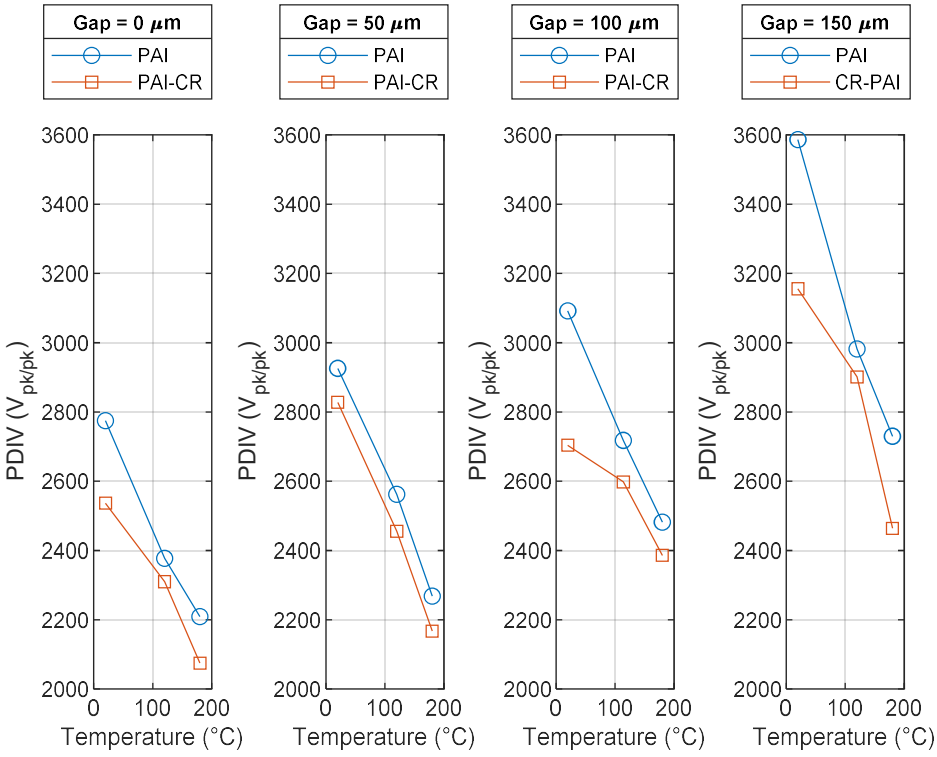

Figure 5-3. PDIV for 110 μm conductors as a function of test temperature and for different gap lengths. Note, gap=0 μm corresponds to the standard back-to-back configuration.

5.5 Insulation thickness 80 μm

Considering that measurements at a temperature of 180°C represent the worst case for PDIV (lowest values), measurements on conductors having the insulation thickness were carried out at 180°C directly. Results are reported in the next section, where the adequacy of the different insulation systems is investigated.

5.6 Evaluation of adequacy of the different conductors

5.7 Fail Criterion

PDIV fail criteria for different DC bus voltages and insulation systems are listed in Table 1. Note that the enhancement factor for temperature is not considered as tests were carried out at 180°C.

Table 5-2.Target values for PDIV. - Phase-to- phase insulation.

Vdc (V)	OF	Aging	PDIV (Vpk-pk) phase-to-phase
800	1.2	1.0	1920
1000	1.2	1.0	2400
1200	1.2	1.0	2880

5.8 Adequacy assessment

The assessment was made considering DC bus voltages of 800 V, 1000 V, and 1200 V. Since PDIV decreases with increasing temperatures (see e.g. Figure 5-1), the assessment of the insulation was made at the maximum operating temperature of 180°C. Therefore, the PDIV values at 180°C for the different conductors and for different gap lengths were reported in Figure 5-4 and Figure 5-5.

It can be concluded that:

- 800 V system: the reliability of phase-to-phase insulation system with 80 μm insulation would be acceptable considering average levels of PDIV. However, when the standard deviation is considered and acceptable reliability levels are considered, the design is never guaranteed, and their usage should be avoided. On the other hand, with an insulation thickness of 110 μm, the insulation systems are always able to support this DC bus level, with higher margin with PAI.
- 1000 V and 1200 V system: there are some instances where certain insulation systems are, on average, able to satisfy requirements, but none can be reliably used.

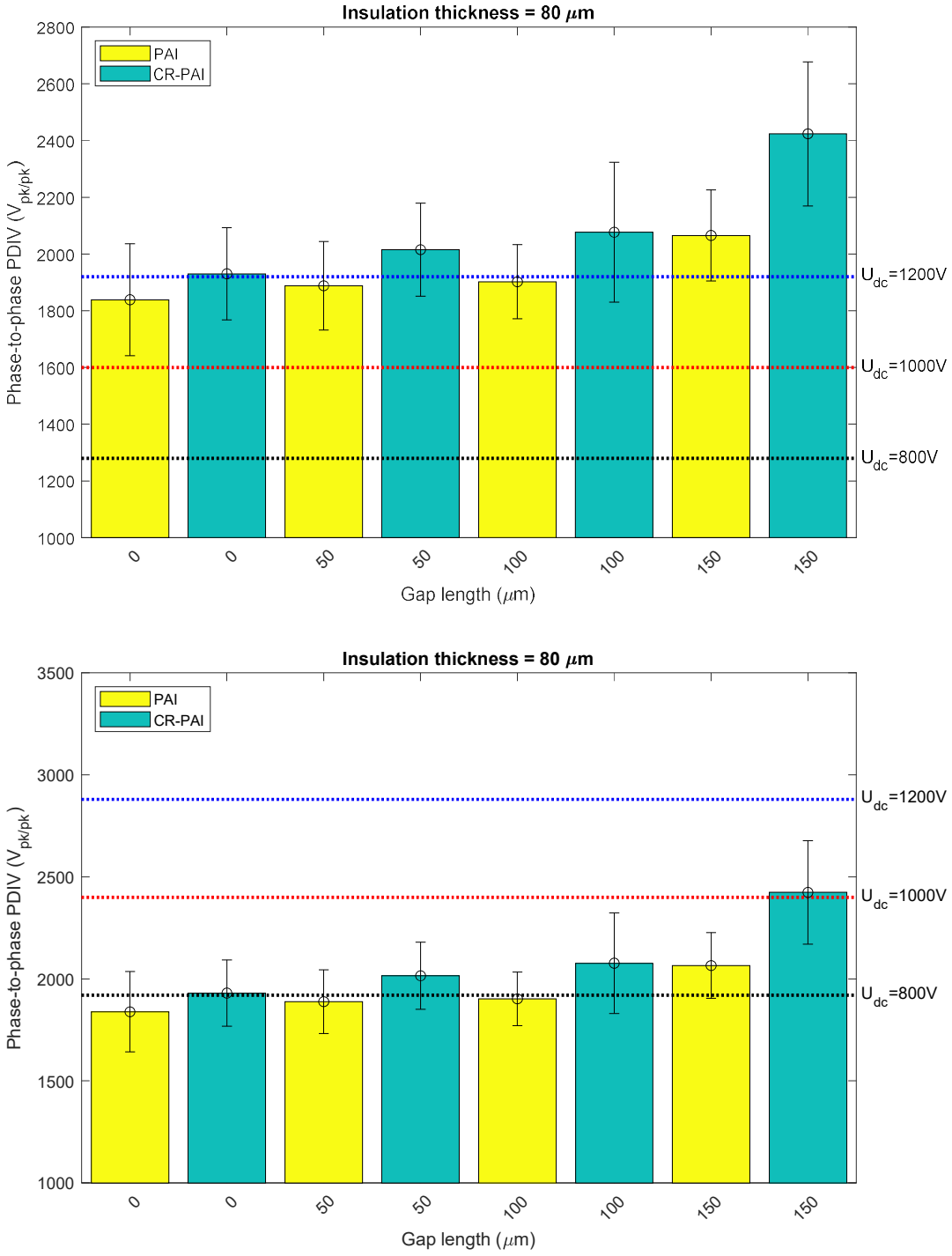

Figure 5-4. PDIV at 180°C and different gap lengths for 80 μm conductors

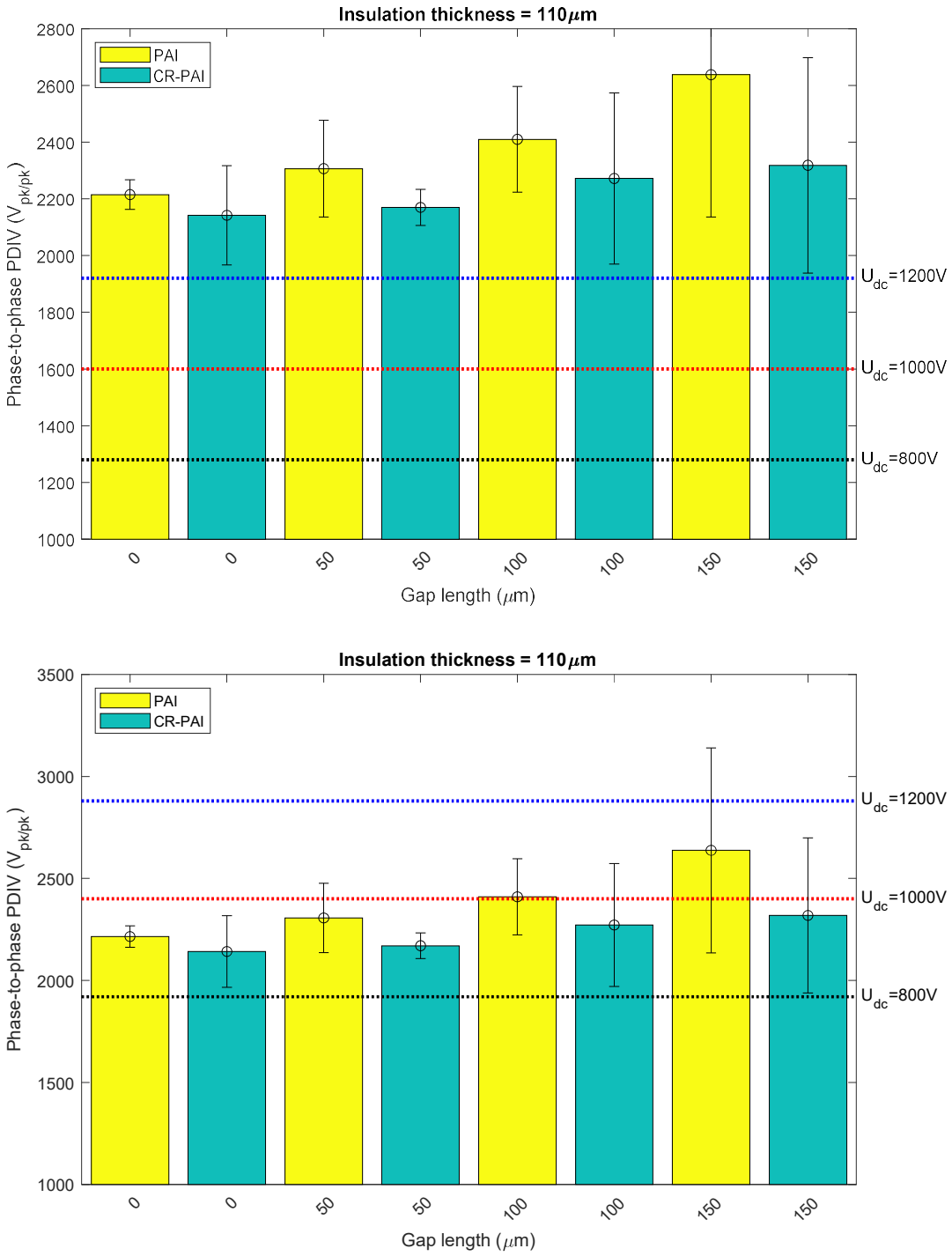

Figure 5-5. PDIV at 180°C and different gap lengths for 110 μm conductors

Table 5-3.Margin (difference between measured PDIV and target values) for the PAI conductors. Phase-to- phase insulation.

Material	Air gap (µm)	Enamel Thickness (mm)	PDIV (Vpk-pk)	Std Dev (V)	Margin – 3*StdDev (Vpk-pk)		
					800 V (1920 Vpp)	1000 V (2400 Vpp)	1200 V (2880 Vpp)
PAI	0	0.11	2215	17	242	-238	-718
	50		2306	57	216	-264	-744
	100		2410	62	304	-176	-656
	150		2638	167	215	-265	-745
	0	0.08	1839	66	-278	-758	-1238
	50		1888	52	-188	-668	-1148
	100		1902	44	-149	-629	-1109
	150		2065	54	-15	-495	-975

Table 5-4.Margin (difference between measured PDIV and target values) for the CR-PAI conductors. Phase-to-phase insulation.

Material	Air gap (µm)	Enamel Thickness (mm)	PDIV (Vpk-pk)	Std Dev (V)	Margin – 3*StdDev (Vpk-pk)		
					800 V (1920 Vpp)	1000 V (2400 Vpp)	1200 V (2880 Vpp)
CR-PAI	0	0.11	2142	58	47	-433	-913
	50		2170	21	187	-293	-773
	100		2272	101	50	-430	-910
	150		2318	127	19	-461	-941
	0	0.08	1930	54	-152	-632	-1112
	50		2015	55	-69	-549	-1029
	100		2077	82	-90	-570	-1050
	150		2424	85	250	-230	-710

6 ASSESSMENT OF PHASE/GROUND INSULATION

6.1 Fail Criterion

PDIV fail criteria for different DC bus voltages and insulation systems are listed in Table 1. Note that the enhancement factor for temperature is not considered as tests were carried out at 180°C.

Table 6-1.Target values for PDIV. - Phase-to- ground insulation.

Udes (V)	OF	Aging	PDIV (Vpk-pk)	
			ph-ph	ph-gnd
800	1.2	1.0	1920	1120
1000	1.2	1.0	2400	1400
1200	1.2	1.0	2880	1680

6.2 Adequacy assessment

The phase-to-ground PDIV was measured using the setup sketched in Figure 6-1. The tests were carried out at 180°C. As can be seen, the conductor is in direct contact with a grounded plane. Thus the model represents:

1. the worst case (absence of over-molding resin)
2. the direct contact with the semi-magnetic wedge used to close the slot.
3. the behavior of the insulation within the linear part of the slot

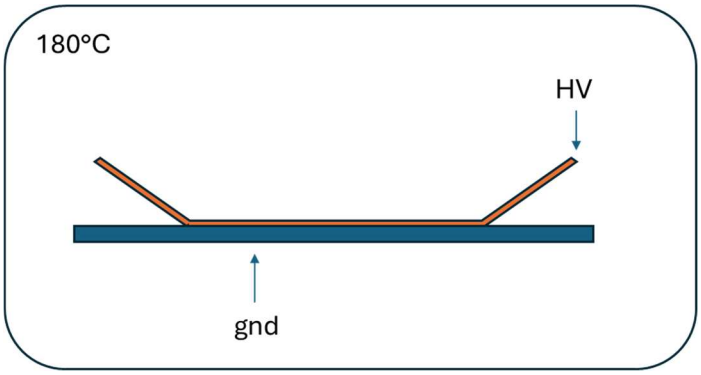

Figure 6-1. Sketch of the model used for testing the phase/ground insulation model

The margins (difference between measured PDIV and target values) are collected in

Table 6-2. It can be concluded that:

- 800V system: the presence of such material in direct contact with conductors does not affect the reliability of phase-to-ground insulation system and its usage could be considered also without the addition of further insulating materials.
- 1000V system: only conductors with an insulation thickness of 110 µm can be used.
- 1200 V system: conductors with an insulation thickness larger than 110 µm are necessary.

Table 6-2.Margin (difference between measured PDIV and target values) for the PAI conductors. Phase-to-ground insulation.

Insulation	PDIV (Vpk-pk)	Margin (Vpk-pk)		
		Udes 800 V	Udes 1000 V	Udes 1200 V
PAI 0.11	1551	431	151	-129
CR-PAI 0.11	1537	417	137	-143
PAI 0.08	1403	283	3	-277
CR-PAI 0.08	1403	283	3	-277

7 ASSESSMENT OF TURN/TURN INSULATION

As a preliminary assessment, it is possible to consider a conservative case, assuming $\rho = 0.3$ (instead $\rho = 0.19$, see Section 11). Under these conditions, the peak-to-peak voltage applied to the turn insulation is:

$$U_{T-T} = 2 \times \frac{2}{3} \times \rho \times (U_{des} + U_b) = 1.6 \times U_{des} \quad (7.1)$$

Under the worst case, the limit values for the peak-to-peak PDIV measured at 180°C and 210°C (thus, it is not needed to consider the enhancement factor for temperature) are:

- 800 V system: 384 $V_{pk/pk}$
- 1000 V system: 480 $V_{pk/pk}$
- 1200 V system: 576 $V_{pk/pk}$

As can be seen from Figure 7-2 and Figure 7-3, even in the worst case (temperature = 210°C), the considered conductors perform satisfactorily for 800 V, 1000V, and 1200V.

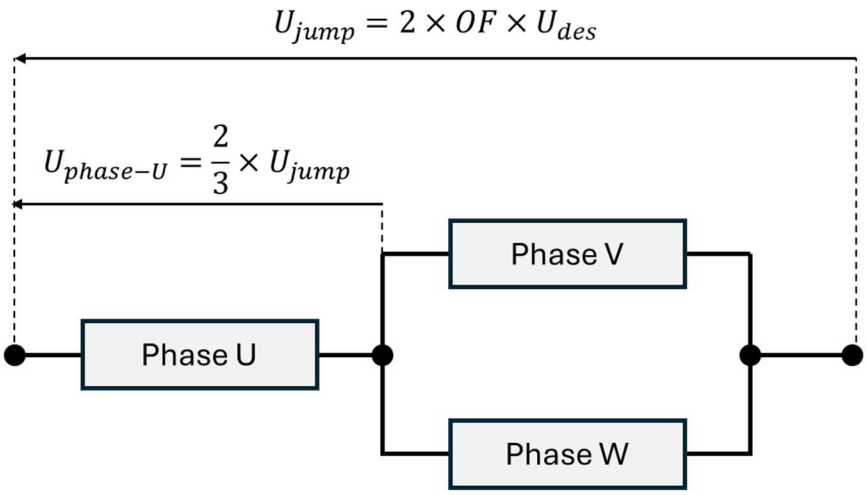

Figure 7-1. Voltages applied to the winding during operation

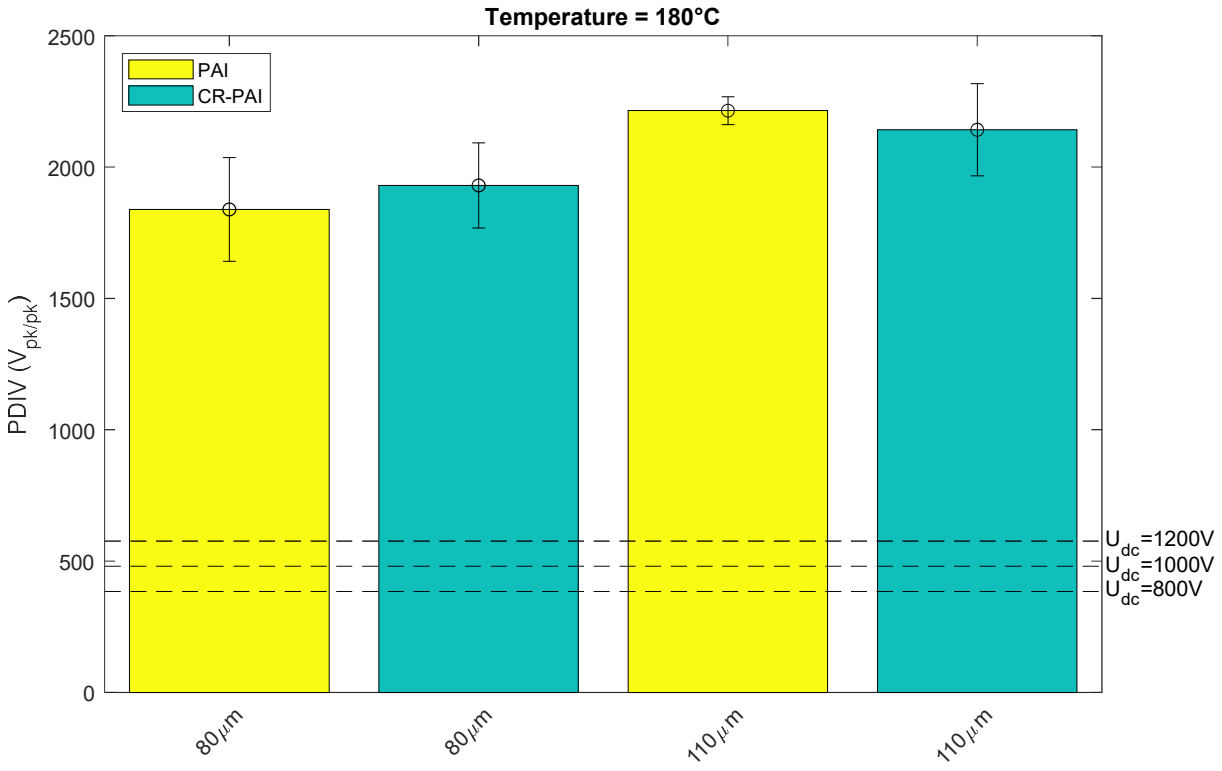

Figure 7-2. PDIV of turn-to-turn insulation models. Temperature= 180°C.

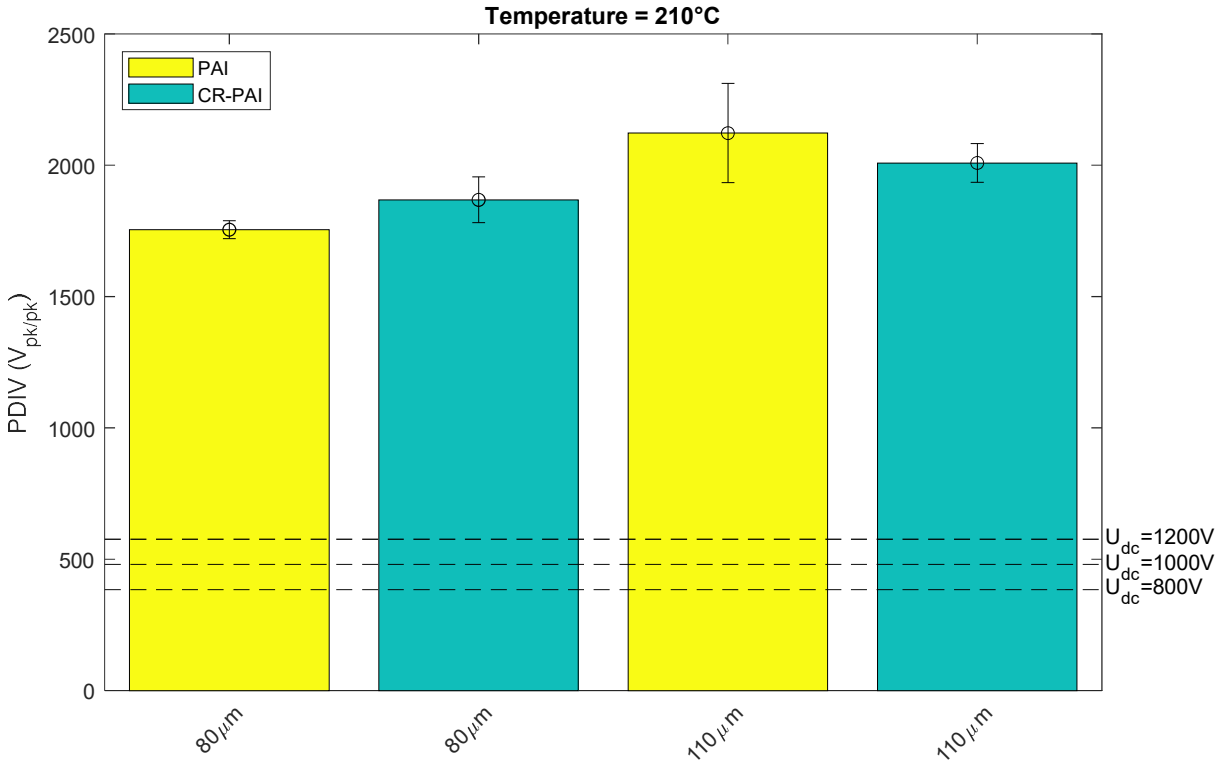

Figure 7-3. PDIV of turn-to-turn insulation models. Temperature= 210°C.

8 CHEMICAL COMPATIBILITY

The chemical compatibility of the automatic transmission fluid (ATF) used for cooling (Castrol ON BOT G5) with the dielectrics used in the HEFT machine was tested by accelerated thermal testing. Insulated conductors having a length of 4 cm approximately were placed in sealed aluminum containers together with the slot molding resin (G720E and XQ8763) in the back-to-back configuration (see Fig.1). The ATF was poured into the containers, covering all the solid insulations. Containers with both the insulated conductors and the resin (hence, without oil) were also prepared for the sake of comparison.

Considering the fire point of the oil (180°C) and the maximum temperature in operation (210°C), the tests were performed at a temperature of 160°C, by placing the test vessels in an oven.

Thermal aging was carried out for two weeks. Dielectric spectroscopy of the conductors and partial discharge inception voltage measurements (PDIV) of the back-to-back samples were carried out prior and after aging. The PDIV measurements were carried out at 20°C, 180°C, and 210°C. In dielectric spectroscopy, electrode contact was guaranteed by directly connecting one electrode to the inner copper conductor and using conductive silver paint to produce a consistent electrical contact between on the outer surface of insulated conductors and the second measurement electrode.

As shown in Fig. 2, an appreciable reduction of the PDIV due to thermal aging could not be observed. Some changes could be observed in the dielectric spectroscopy (Fig. 3 and Fig. 4), with the resin G720E giving rise to a dissipation factor peak at low frequency (10 Hz), The XQ8763 resin, on the contrary, gave rise to a loss peak at some hundreds of kHz.

The most concerning result came from visual inspection, since after aging the insulation tended to separate from the conductor, as shown in Fig. 5.

One of the possible explanations for conductor/insulation delamination was the presence of corrosive sulfur in the ATF. This phenomenon was discovered in transformers and was associated to the use of an additive with anti-oxidation properties, the dibenzyl disulfide (DBDS). DBDS can corrode the copper forming copper sulfide (Cu_2S). Therefore, a test similar to what proposed to discover the presence of corrosive sulfur in transformer oils was used for the ATF. The test consists in wrapping bare copper conductors with kraft paper, immerse the samples in oil, and age at 140°C for four days. Oils with corrosive sulfur give rise to visible traces of Cu_2S in the paper. The same test was also carried out at a temperature of 160°C, that is the temperature at which the chemical compatibility tests were made. The results of both tests did not support the hypothesis that corrosive sulfur was the root cause for delamination: copper sulfide could not be observed in the paper, nor the Fourier Transform InfraRed (FTIR) analysis could evidence anomalies.

It was decided to test conductors at 220°C (their class temperature), in air, for one week. In these tests, the conductors were placed in the oven without resins or ATF. The results are shown in Fig. 6. A massive enamel/conductor separation can be observed. These findings suggest the following:

1. Separation is probably due to enamel issues (inadequate adhesion, or a thermal expansion coefficient not matching that of the copper).
2. Otherwise, polyamide-imide did not show substantial changes in the PDIV due to aging in the presence of ATF and resins.
3. The increase of dissipation factor at 10 kHz observed during chemical compatibility tests using the XQ8763 resin is potentially a threat for the insulation reliability (excessive temperature, thermal runaway in the worst case).

Therefore, the decided course of action is to procure insulated conductors without the issues observed before and re-test chemical compatibility, with special care for dielectric spectroscopy. Should the increase of the dissipation factor during tests with XQ8763 be confirmed, this resin will be discarded.

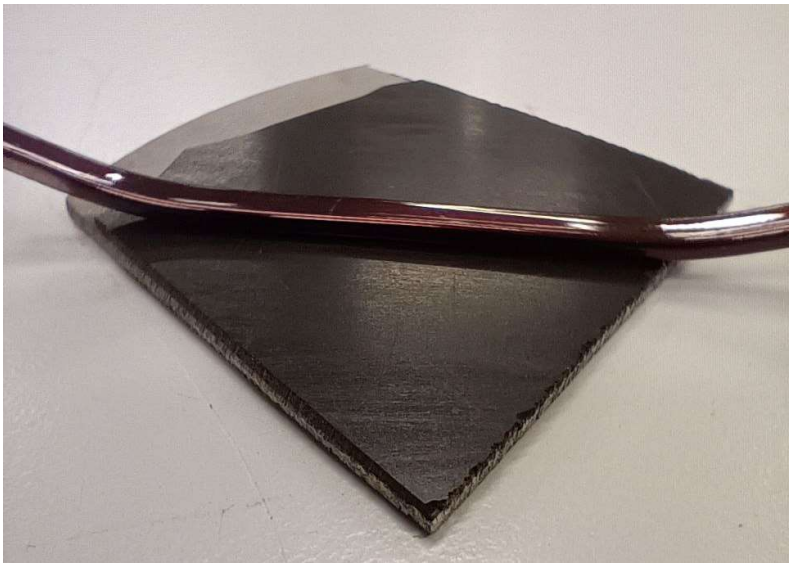

Figure 8-1. Insulated conductor and slot molding resin in the back-to-back configuration

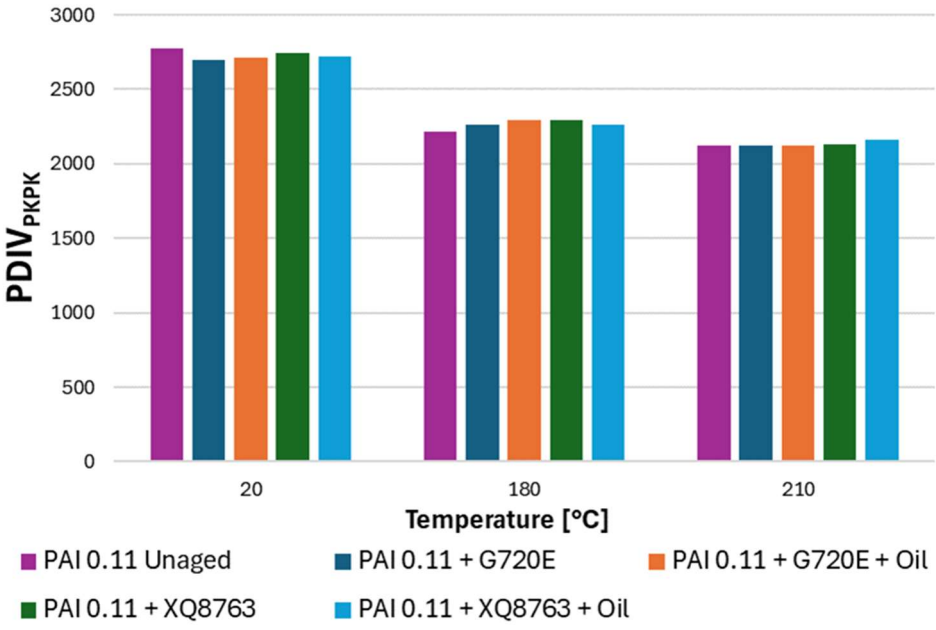

Figure 8-2. Results of PDIV measurements

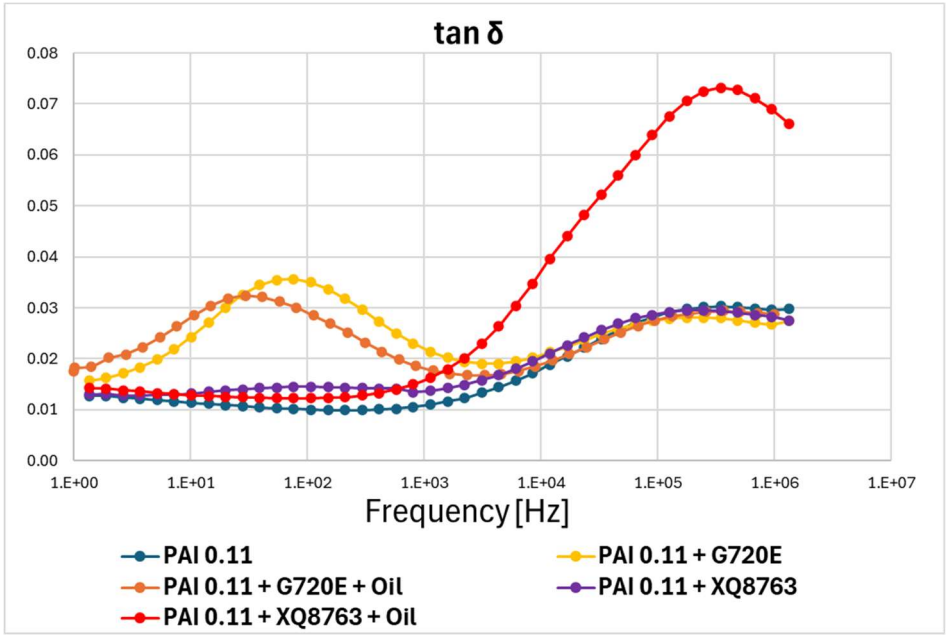

Figure 8-3. Results of dielectric spectroscopy performed on back-to-back samples: dissipation factor (tanδ).

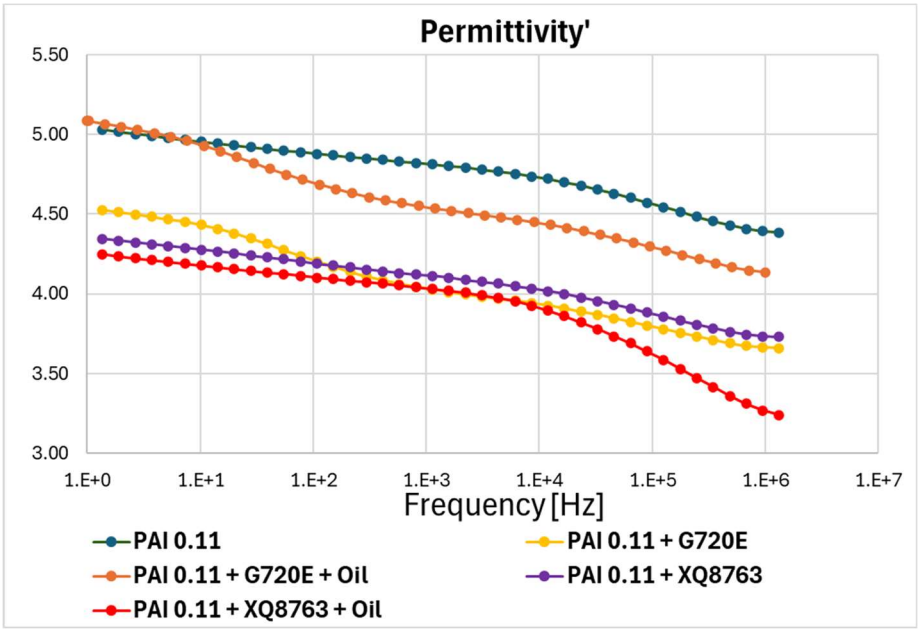

Figure 8-4. Results of dielectric spectroscopy performed on back-to-back samples: real part of permittivity (ε')

Figure 8-5. Evidence of conductor/insulation separation during the chemical compatibility tests

Figure 8-6. Evidence of conductor/insulation separation during tests at 220°C for one week.

9 DELIVERY DEVIATIONS FROM THE INITIAL PLANNING

There has been a delay in the delivery of D2.4. Analysis and validation of machine insulation for 800V DC bus

Contractual delivery: 2024-03-31

Deliverable Date: 2024-06-21

This delay is due to:

The lubricant oil (Castrol ON BOT (BEV) G5) used also for cooling by spraying it on the end-windings could not be purchased in Italy. Provisions were made to get 10 liters directly from Castrol, but until the mid of March it was not received by UNIBO.

Administrative deviations:

First draft of the document was uploaded to the TEAMS platform in March, there was a delay in the reception of the lubricant oil needed for last tests, which has delay the final version of document. This delay in the deliverable submission does not entail delays in other tasks.

10 CONCLUSIONS

The insulation system proposed for the HEFT motor will be suitable for a 800 Vdc machine using either PAI or CR-PAI conductors (the latter has a somewhat worse performance probably due to the content of nanoparticles that increase the permittivity). The suggested thickness for the conductor insulation is 110 μm. Conductors with enamel 80 μm-thick do not ensure that the stator remains partial discharge free in operation since they exhibit insufficient partial discharge inception voltage in the phase-to-phase insulation of the end-winding.

The use of advanced resins for stator slot molding is an interesting proposal for improving heat transmission capabilities. Their performance in the frequency range used by EVs is a bit worse than that of conventional liners (higher permittivity), especially considering the resin with larger filler content and better thermal conductivity. Despite this, conductors with an enamel 110 μm-thick ensure sufficient margin for reliable operation as tests performed using a grounded plane without any coating show that the enamel thickness ensures a partial discharge inception voltage that is above the applied phase-to-ground voltage.

Systems with higher voltages will require different arrangements. The margins for the phase-to-phase and phase-to-ground insulation are not sufficient. Unfortunately, despite the fact that the turn-to-turn insulation does not pose concerns, higher insulation thicknesses will be required for the conductors.

11 APPENDIX CALCULATIONS FOR TURN-TO-TURN VOLTAGES

The turn voltage calculations were based on the procedure described in [4]. The model was derived using FEA tools to derive the parameters of the equivalent circuit reported in Figure 11-1. In particular, the following steps were carried out:

1. Calculate the capacitance matrix, **C**, for the conductors within the slot. The model for the HEFT slot is reported in

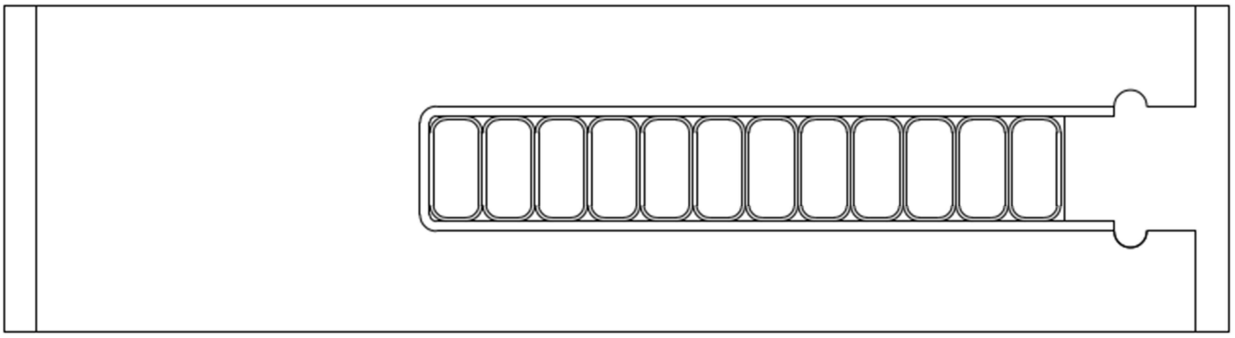

2. Figure 11-2.
3. Calculate the inductance matrix, **L**, of the conductors in the slot. Considering the frequency of the voltage applied to the coil, a reference frequency of 10 MHz was considered.
4. From the previous calculation, the resistance matrix of the conductors in the slot (reference frequency also here is 10 MHz).

The next step was the calculation of the response to an impulsive voltage waveform of the equivalent circuit reported in Figure 11-1. To solve the circuit in compact form, the connectivity matrix in eqn. (12.1) is first defined.

$$\mathbf{D}=\begin{pmatrix}-1 & 0 & 0 & \cdots & 0\\ 1 & -1 & 0 & \cdots & 0\\ 0 & 1 & -1 & \cdots & 0\\ \cdots & \cdots & \cdots & \ddots & 0\\ 0 & 0 & 0 & \cdots & 1\end{pmatrix} \tag{12.1}$$

This allows to write the Kirchoff's laws in compact form. The Kirchoff's voltage current and voltage laws are expressed using the matrices **D**, **C**, and **L** in equations (12.2) and (12.3), respectively.

$$-\mathbf{D}^T\mathbf{i}=\mathbf{C}\frac{d\mathbf{v}}{dt} \tag{12.2}$$

$$v_{in}-\mathbf{D}\cdot\mathbf{v}=\mathbf{R}\cdot\mathbf{i}+\mathbf{L}\frac{d\mathbf{i}}{dt} \tag{12.3}$$

Where **i** is the vector of the currents in each inductive branch, and **v** is the vector of the turn to ground voltages. After some manipulations, the equations (12.4) and (12.5) are derived.

$$\frac{d\mathbf{v}}{dt}=-\mathbf{C}^{-1}\mathbf{D}^T\mathbf{i} \tag{12.4}$$

$$\frac{d\mathbf{i}}{dt}=\mathbf{L}^{-1}\left(v_{in}+\mathbf{D}\cdot\mathbf{v}-\mathbf{R}\cdot\mathbf{i}\right)+ \tag{12.5}$$

These equations can be implemented using e.g. Simulink using the model shown in Figure 11-3.

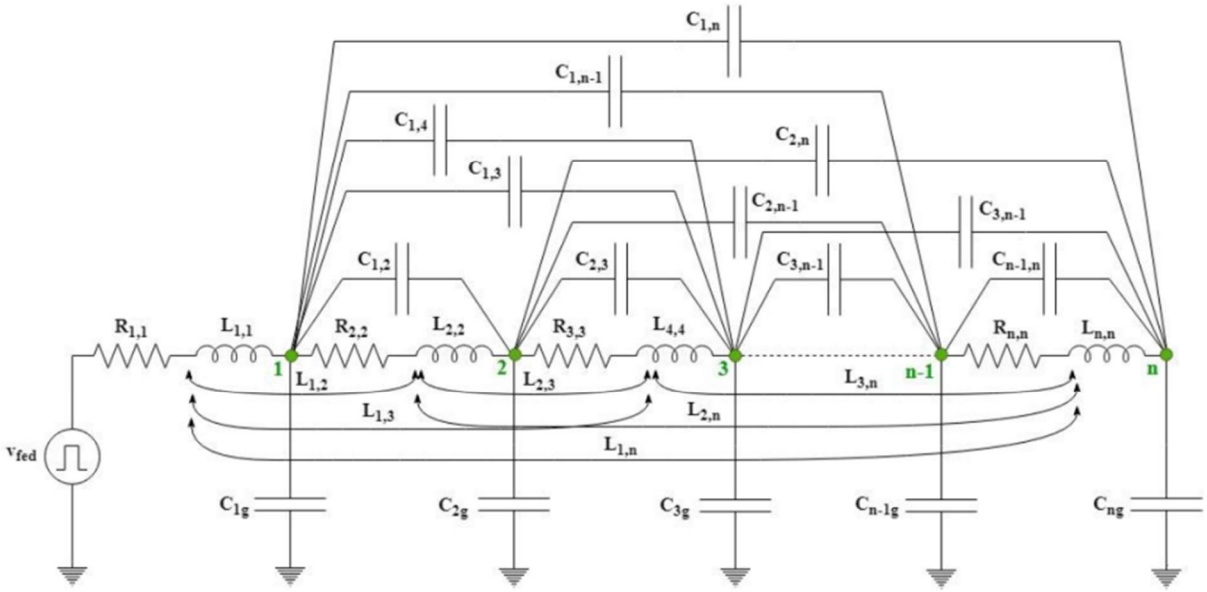

Figure 11-1. Reference concentrated-parameter model

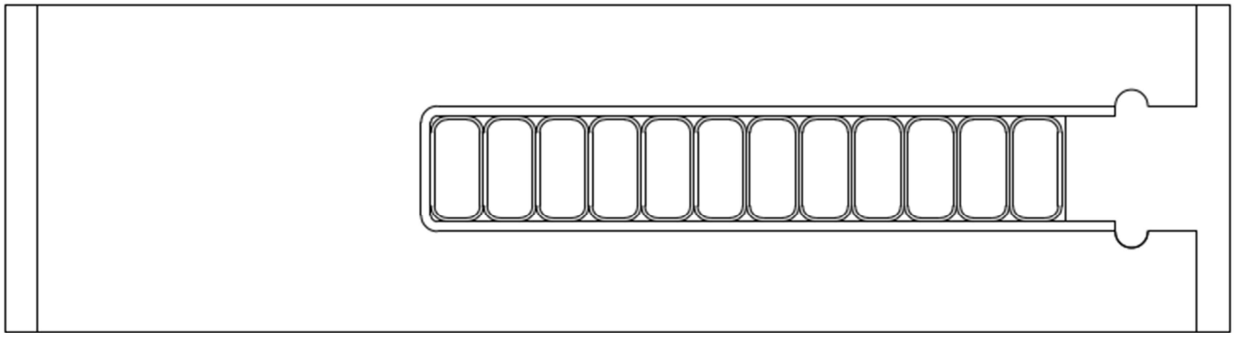

Figure 11-2. Slot model for FEA

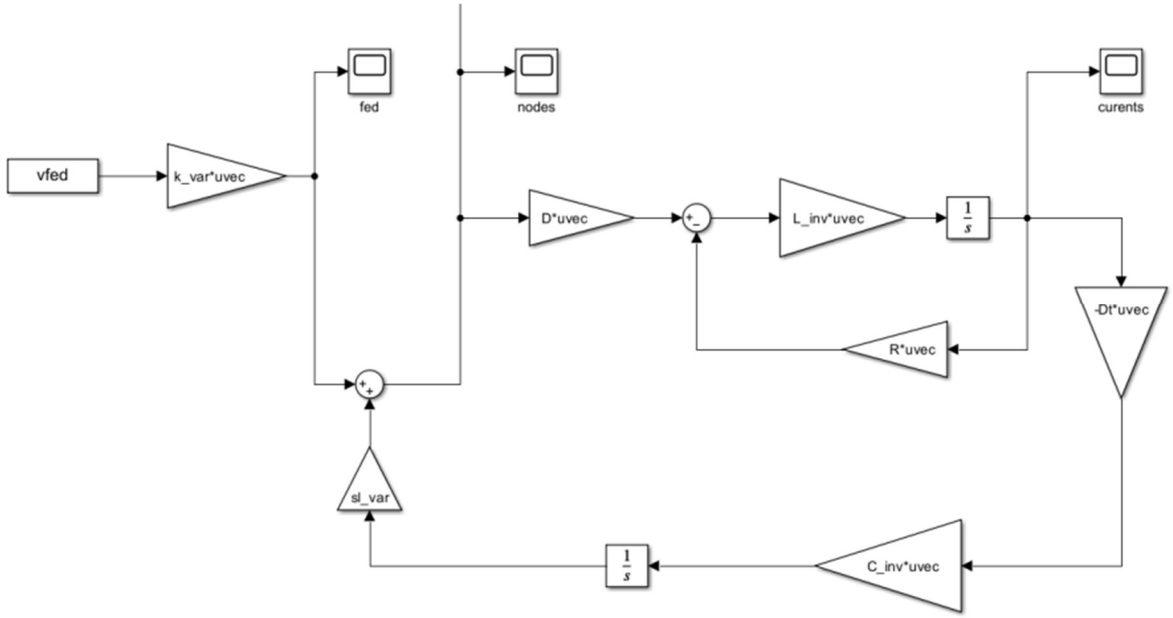

Figure 11-3. Dynamic simulation model. L is the inductance matrix, C the capacitance matrix, R the resistance matrix, D the turn connectivity matrix.

11.1 Results

Simulations were carried out using the following parameters:

1. Conductor size
    a. Height: 1.39 mm
    b. Width: 3.02 mm
    c. Fillet radius: 0.4 mm
2. Stator length: 65 mm
3. Enamel thickness: 110 μm
4. Enamel relative permittivity: 3.7
5. Resin thickness: 300 μm (expected value)
6. Resin relative permittivity: 5.8 (worst case)

The capacitance, inductance and resistance matrices derived using FEA are reported in Table 11-1, Table 11-2, and Table 11-3. The turn voltages derived from the simulations are reported in Figure 11-4. In order to clarify the results, Figure 11-5 and Figure 11-6 report the turn voltages and the potential difference between adjacent voltages using colormaps. Unexpectedly, the worst case does not seem to be the potential difference between turns 1 and 2, but that between turns 10 and 11, equal to 18.6 for an input voltage of 100 V. This value corresponds to a ρ=0.186~0.19 in Table 3-2.

Table 11-1. Capacitance matrix (pF)

	1	2	3	4	5	6	7	8	9	10	11	12
1	819	-369	0	0	0	0	0	0	0	0	0	0
2	-369	950	-369	0	0	0	0	0	0	0	0	0
3	0	-369	950	-369	0	0	0	0	0	0	0	0
4	0	0	-369	950	-369	0	0	0	0	0	0	0
5	0	0	0	-369	950	-369	0	0	0	0	0	0
6	0	0	0	0	-369	950	-369	0	0	0	0	0
7	0	0	0	0	0	-369	950	-369	0	0	0	0
8	0	0	0	0	0	0	-369	950	-369	0	0	0
9	0	0	0	0	0	0	0	-369	951	-369	0	0
10	0	0	0	0	0	0	0	0	-369	951	-369	0
11	0	0	0	0	0	0	0	0	0	-369	950	-369
12	0	0	0	0	0	0	0	0	0	0	-369	776

Table 11-2. Inductance matrix (nH)

	1	2	3	4	5	6	7	8	9	10	11	12
1	58.5	27.4	12.8	6.0	2.8	1.3	0.6	0.3	0.1	0.1	0.0	0.0
2	27.4	61.0	28.6	13.4	6.3	2.9	1.4	0.6	0.3	0.1	0.1	0.0
3	12.8	28.6	61.6	28.9	13.5	6.3	3.0	1.4	0.7	0.3	0.1	0.0
4	6.0	13.4	28.9	61.9	29.0	13.6	6.4	3.0	1.4	0.6	0.3	0.1
5	2.8	6.3	13.5	29.0	61.8	29.0	13.6	6.4	3.0	1.4	0.6	0.2
6	1.3	2.9	6.3	13.6	29.0	61.9	29.0	13.6	6.3	2.9	1.3	0.5
7	0.6	1.4	3.0	6.4	13.6	29.0	61.8	28.9	13.5	6.3	2.8	1.0
8	0.3	0.6	1.4	3.0	6.4	13.6	28.9	61.7	28.9	13.4	5.9	2.1
9	0.1	0.3	0.7	1.4	3.0	6.3	13.5	28.9	61.6	28.6	12.7	4.4
10	0.1	0.1	0.3	0.6	1.4	2.9	6.3	13.4	28.6	61.0	27.0	9.4
11	0.0	0.1	0.1	0.3	0.6	1.3	2.8	5.9	12.7	27.0	57.7	20.1
12	0.0	0.0	0.0	0.1	0.2	0.5	1.0	2.1	4.4	9.4	20.1	43.0

Table 11-3. Resistance matrix (Ω)

	1	2	3	4	5	6	7	8	9	10	11	12
1	0.444	Inf	Inf	Inf	Inf	Inf	Inf	Inf	Inf	Inf	Inf	Inf
2	Inf	0.440	Inf	Inf	Inf	Inf	Inf	Inf	Inf	Inf	Inf	Inf
3	Inf	Inf	0.441	Inf	Inf	Inf	Inf	Inf	Inf	Inf	Inf	Inf
4	Inf	Inf	Inf	0.429	Inf	Inf	Inf	Inf	Inf	Inf	Inf	Inf
5	Inf	Inf	Inf	Inf	0.438	Inf	Inf	Inf	Inf	Inf	Inf	Inf
6	Inf	Inf	Inf	Inf	Inf	0.429	Inf	Inf	Inf	Inf	Inf	Inf
7	Inf	Inf	Inf	Inf	Inf	Inf	0.432	Inf	Inf	Inf	Inf	Inf
8	Inf	Inf	Inf	Inf	Inf	Inf	Inf	0.447	Inf	Inf	Inf	Inf
9	Inf	Inf	Inf	Inf	Inf	Inf	Inf	Inf	0.439	Inf	Inf	Inf
10	Inf	Inf	Inf	Inf	Inf	Inf	Inf	Inf	Inf	0.443	Inf	Inf
11	Inf	Inf	Inf	Inf	Inf	Inf	Inf	Inf	Inf	Inf	0.504	Inf
12	Inf	Inf	Inf	Inf	Inf	Inf	Inf	Inf	Inf	Inf	Inf	0.737

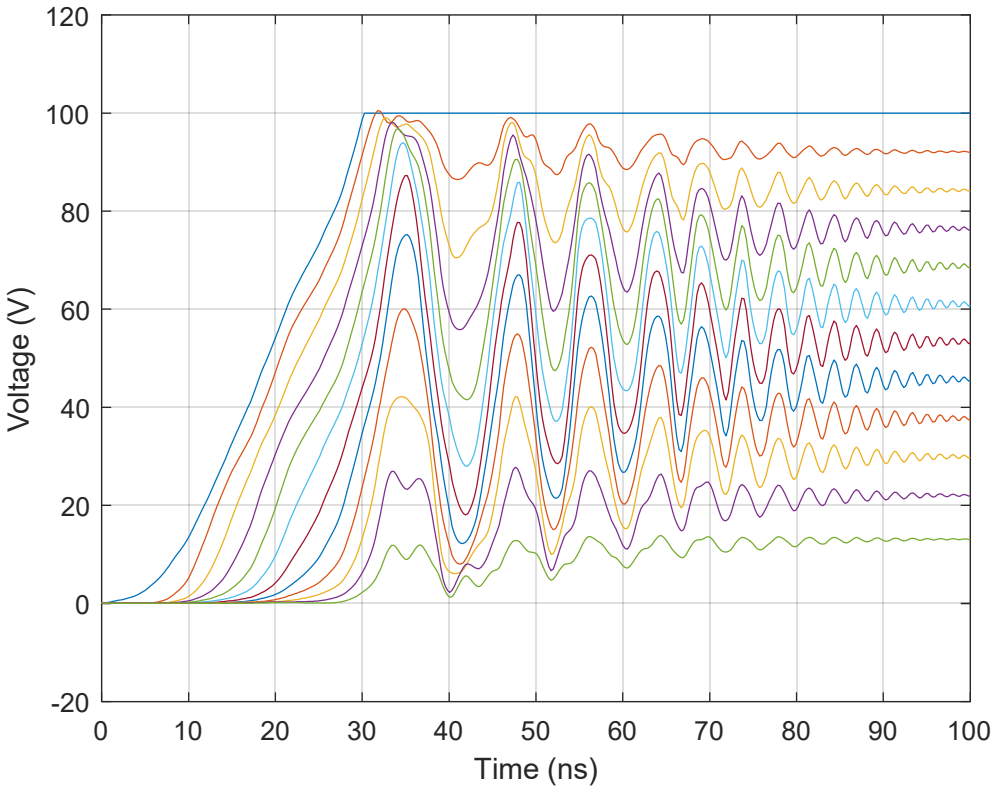

Figure 11-4. Simulation of turn voltages (input: 100V surge with 30 ns rise time)

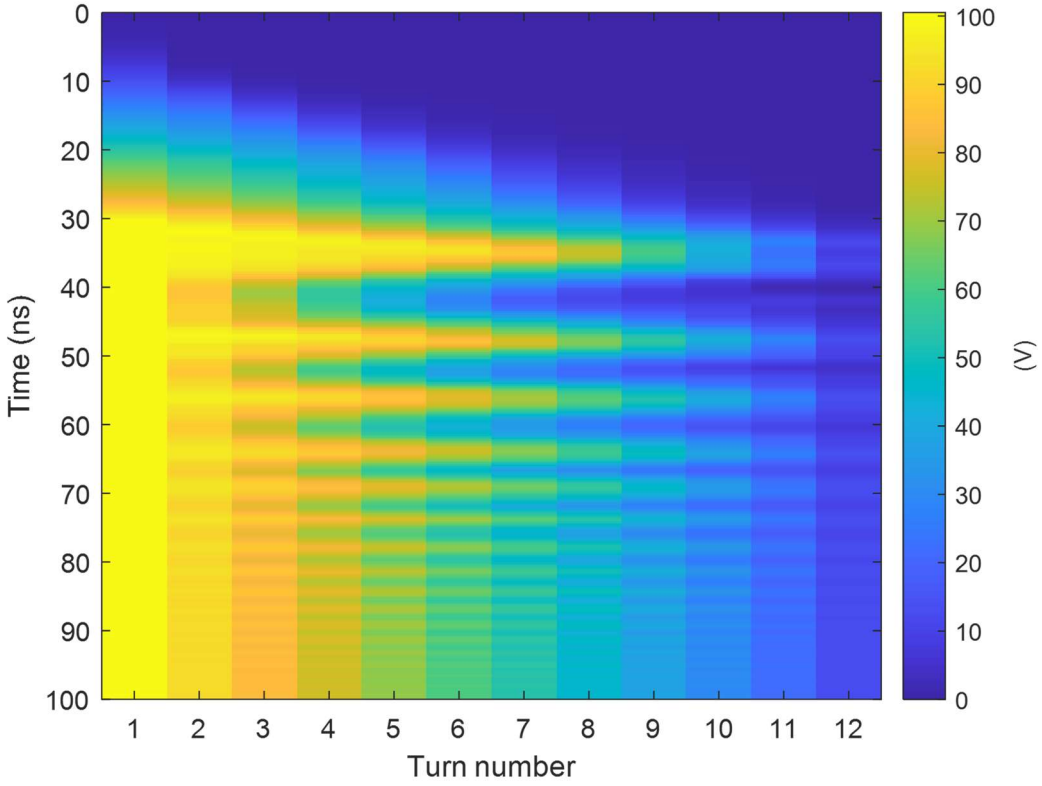

Figure 11-5. Colormap showing the turn voltages (input: 100V surge with 30 ns rise time)

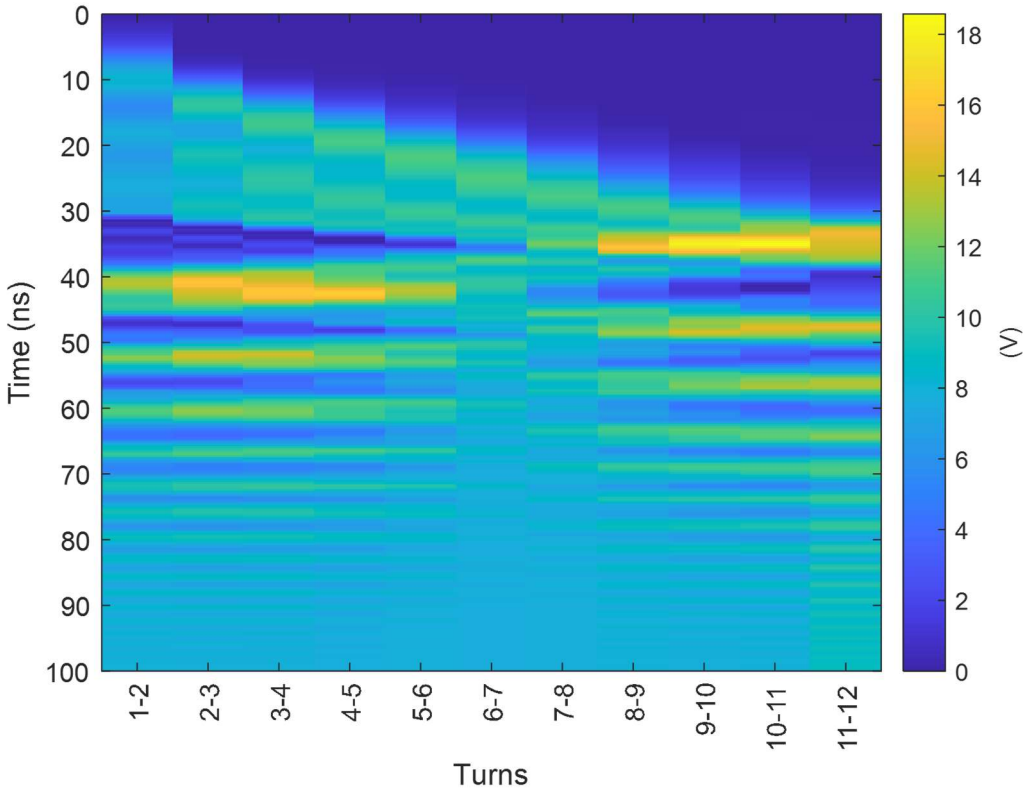

Figure 11-6. Colormap showing the potential differences between adjacent turns (input: 100V surge with 30 ns rise time)